Stabilization and Structural Alteration of the G-Quadruplex DNA Made from the Human Telomeric Repeat Mediated by Tröger's Base Based Novel Benzimidazole Derivatives

Ananya Paul,[†] Basudeb Maji,[†] Santosh K. Misra,[†] Akash K. Jain,[†] K. Muniyappa,[‡] and Santanu Bhattacharya*[,†,§]

[†]Department of Organic Chemistry and [‡]Department of Biochemistry, Indian Institute of Science, Bangalore 560 012, India
[§]Chemical Biology Unit, Jawaharlal Nehru Centre for Advanced Scientific Research, Bangalore 560 012, India

Ⓢ Supporting Information

ABSTRACT: Ligand-induced stabilization of the G-quadruplex DNA structure derived from the single-stranded 3′-overhang of the telomeric DNA is an attractive strategy for the inhibition of the telomerase activity. The agents that can induce/stabilize a DNA sequence into a G-quadruplex structure are therefore potential anticancer drugs. Herein we present the first report of the interactions of two novel bisbenzimidazoles (**TBBz1** and **TBBz2**) based on Tröger's base skeleton with the G-quadruplex DNA (G4DNA). These Tröger's base molecules stabilize the G4DNA derived from a human telomeric sequence. Evidence of their strong interaction with the G4DNA has been obtained from CD spectroscopy, thermal denaturation, and UV–vis titration studies. These ligands also possess significantly higher affinity toward the G4DNA over the duplex DNA. The above results obtained are in excellent agreement with the biological activity, measured in vitro using a modified TRAP assay. Furthermore, the ligands are selectively more cytotoxic toward the cancerous cells than the corresponding noncancerous cells. Computational studies suggested that the adaptive scaffold might allow these ligands to occupy not only the G-quartet planes but also the grooves of the G4DNA.
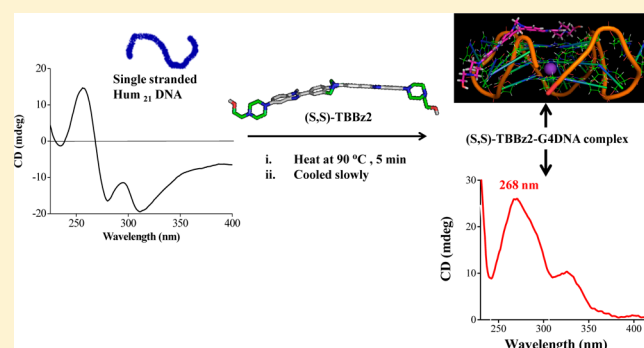
■ INTRODUCTION

Human telomeres, which occur in the 3′-ends of human chromosomal DNA, consist of hexanucleotide repeats, i.e., 5′-TTAGGG-3′. Telomerase enzyme is a ribonucleoprotein, which protects the telomeres from damage to ensure end-to-end recombination upon addition of the hexanucleotide repeats.[1−3] There are fundamental differences between the telomere maintenance in the somatic cells compared to that in the cancer cells. The progressive shortening of the telomeres in the former eventually leads to senescence and apoptosis.[4] In contrast the cancer cells are immortal because their telomere lengths are maintained by the telomerase enzyme.[4,5] Telomerase is overexpressed in 85−90% of the human tumor cells and has undetectable activity in most of the normal somatic cells.[4,5] Thus, the telomerase represents an attractive target with good selectivity for the tumor cells over the healthy tissues, and the telomerase inhibition has been identified as a powerful approach to modern cancer therapy.[6−8] Telomerase can be inhibited by folding the telomeric overhangs into the four-stranded G4DNA structures, which do not serve as a substrate for the telomerase.[9,10] In addition G4DNA formation may dissociate telomere ends from physical association with the telomerase and other telomere-binding protein,[9] which in cells

then results in the triggering of a DNA damage response and eventual cell death.[10]

Thus, the design and synthesis of new G-quadruplex ligands, which induce the folding of guanine rich DNA into the G4DNA structures, are important research activities for medicinal chemists interested in anticancer drug design. To date, a number of families of G-quadruplex ligands have been identified and studied for their G4DNA stabilization and telomerase inhibition properties.[11−15] Most of the G-quadruplex ligands possess a large planar aromatic chromophore by which they can interact with the planar G-quartet surface of a G-quadruplex via $\pi−\pi$ stacking interactions. Another class of ligands, which do not have extended heteroaromatic chromophore for $\pi−\pi$ interactions, can stabilize the G4DNA through groove or loop binding. These include oligopeptides (netropsin, distamycin-A, etc.), benzimidazoles, carbocyanine dyes, etc.[2,13,15−19]

In 1887, Tröger first synthesized a methanodibenzo[1,5]-diazocin structure (compound **1**) (Figure 1) via the aromatic electrophilic substitution of *p*-anisidine with formaldehyde.[20]
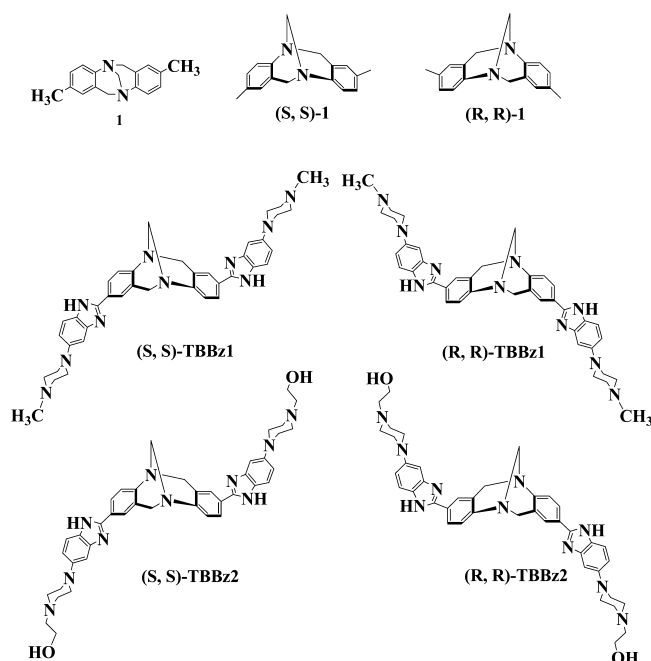
Figure 1. Chemical structures of the Tröger's base (**1**) and the ligands used in this study, **TBBz1** and **TBBz2**.

Later, this compound, which is a chiral amine with two stereogenic nitrogen centers, was named Tröger's base. The unique set of structural features, for instance, the C_2-symmetric heterocyclic and rigid framework, folded-geometry with a plane of aromatic rings almost perpendicular to each other, and hydrophobic cavity, makes the Tröger's base derivatives attractive targets for applications in molecular recognition studies of substrates having specific shapes or conformation.[21] Recently many analogues of Tröger's base have been used as a host in recognition phenomena,[22] DNA interaction,[23−25] and enzyme inhibition[26] and as ligands for asymmetric catalysis.[27] Thus, the use of Tröger's base as a scaffold for the generation of G-quadruplex binding ligand is an appropriate endeavor given that Tröger's base derivatives have been shown to bind to other DNA forms.

Earlier we have shown the stabilization, topology alteration, and induction (in the absence of any added cations) of the G4DNA derived from the sequence $d(T_2G_4)_4$[28,29] and human telomeric repeat $d[G_3(T_2AG_3)_3]$ and $d(T_2A\ G_3)_8$[30,31] by a series of "V"-shaped symmetrical ligands based on 1,3-phenylene-bis(piperazinyl benzimidazole), which have higher affinity for the G4DNA over the duplex DNA. Herein we describe the first synthesis of two new ligands, based on the Tröger's base scaffold, substituted by the benzimidazole system possessing piparazine side chains. We have chosen here for study a G4DNA that is formed by a human telomeric sequence $d[G_3(T_2AG_3)_3]$. This G4DNA is capable of forming intramolecular conformations stabilized by either K^+ or Na^+ ions.[32−35] We discuss the comparative formation, stabilization, structural alteration, and computational aspects of the G4DNA derived from $d[G_3(T_2AG_3)_3]$ (Hum$_{21}$) in the presence of each of these ligands. We also report the relative efficiency of each ligand toward the inhibition of the telomerase activity as indicated from the modified telomerase repeat amplification protocol (TRAP-LIG) assay and selective cytotoxicity of these molecules toward the cancer cells against the corresponding normal cells.

RESULTS AND DISCUSSION

The benzimidazole moiety resembles the purine bases of natural DNA, and a number of benzimidazole compounds are known to be permeable across the cell and nuclear membranes.[36,37] Some of these are also used in cytometry, chromosomal staining, radioprotection, and enzymatic inhibition and to stabilize various DNA structures, e.g., duplex DNA, triplex DNA, and G4DNA.[18,19,36−41] Tröger's base moiety, on the other hand, has been used frequently for achieving small molecule recognition, design of artificial receptors, and other applications.[22−29] Consequently we synthesized two bisbenzimidazole substituted Tröger's base scaffolds (**TBBz1** and **TBBz2**, Figure 1) having significant bends. To synthesize **TBBz1** and **TBBz2**, we first generated the key dialdehyde (**3**, Scheme 1), starting from the commercially available *p*-aminoethyl benzoate (**1**, Scheme 1). Dialdehyde **3** was then reacted with the freshly synthesized diamine individually (**6** or **7**)[28] under oxidative conditions to afford either **TBBz1** or **TBBz2** (Scheme 1).

Racemic mixtures of many Tröger's base derivatives have been resolved using classic crystallization and separation of diastereomers or using chiral column chromatography.[42,43] However, such attempts with either **TBBz1** or **TBBz2** did not result in satisfactory resolution (not shown). We then tried to resolve each Tröger's base derivative **TBBz1** or **TBBz2** via the preparation of hydrogen bonded, acid−base salt aggregates by using dibenzoyl-(+)-tartaric acid (DBTA).[42] But this attempt at resolution also did not result in complete resolution, although we obtained enrichment of the (+)-enantiomer on both instances, as evident from the circular dichroic spectral data of the ligands (Figure S3 and Figure S14 of Supporting Information). Lack of complete resolution could be due to the fast equilibration between the diastereomeric complexes formed in the solution phase, as reported earlier for the corresponding amide, triazine, and proflavine−phenanthroline based Tröger's base derivatives.[43,44]

Earlier even with the racemic forms of other Tröger's base derivatives, there are reports of specific molecular recognition of duplex DNA by such mixtures.[23,45] Accordingly we decided to go ahead with the above ligands for investigating their G4DNA targeting ability. Monovalent ions such as Na^+ and K^+ induced and stabilized the G4DNA structures. While Li^+ ions induced G4DNA formation, they exerted very little effect on the G4DNA stability.[45] In Na^+ solution, the sequence $d[AG_3(T_2AG_3)_3]$ folds intramolecularly into a G4DNA structure stabilized by three stacked G-tetrads that are connected by two lateral loops and a central diagonal loop leading to an antiparallel geometry.[32] The favored conformation under physiological K^+ solution has mixed parallel/antiparallel strands within the G4DNA.[34−36,46] We used four buffer systems, one of them has $LiCl + Na^+$ (10 mM sodium cacodylate having 100 mM LiCl and 0.1 mM EDTA, pH 7.4), and the other three contained LiCl or NaCl or KCl salts (10 mM Tris-HCl having 100 mM LiCl or NaCl or KCl and 0.1 mM EDTA, pH 7.4). We used heat annealing conditions to form the G4DNA derived from the sequence $d[G_3(T_2AG_3)_3]$ (abbreviated as Hum$_{21}$) (see Materials and Methods).

The CD spectra of the G4DNA formed by Hum$_{21}$ in NaCl and KCl are similar to those reported earlier (Figure 2).[35,36] The G4DNA formed in KCl solution has one small negative peak near 240 nm, a positive peak near 290 nm, and shoulders near 250 and 270 nm, similar to those reported for the human

Scheme 1[a]
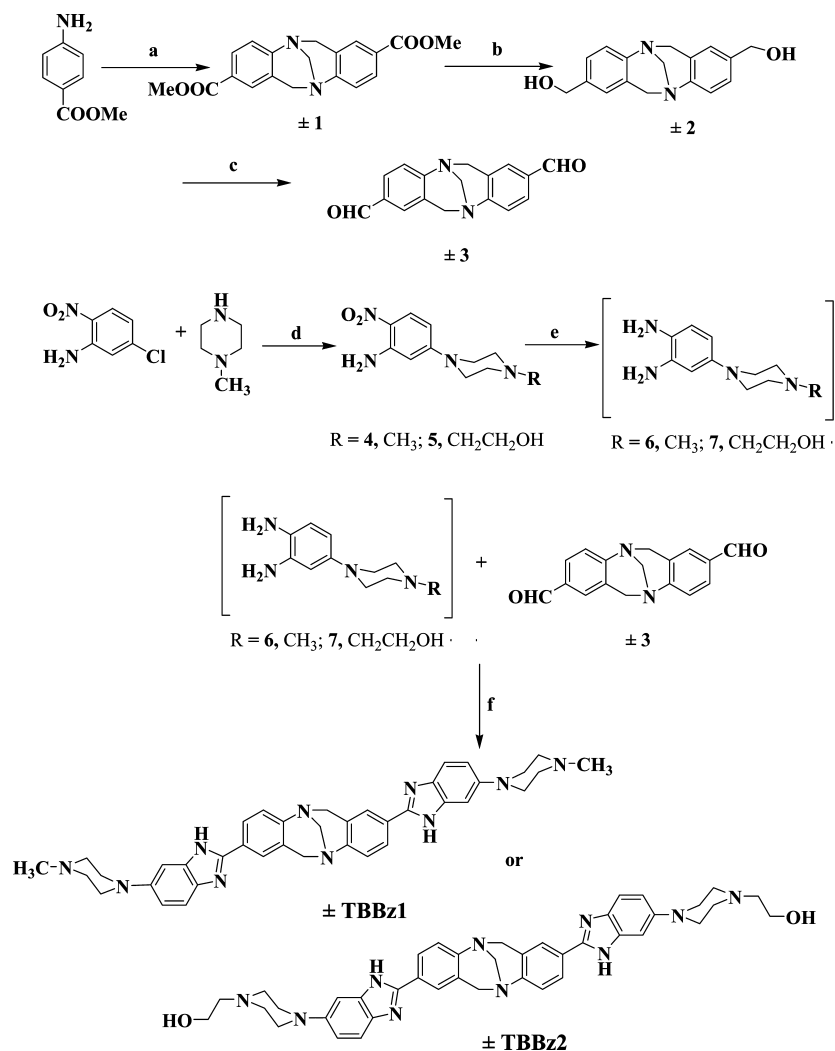
[a]Reagents, conditions, and yields: (a) TFA, paraformaldehyde, reflux, rt, 48 h (58%); (b) LAH, dry THF, rt, 15 h (80%); (c) PCC, THF, rt, 10 h (85%); (d) DMF, 120 °C, 24 h (80%); (e) MeOH, Pd−C (10%), H$_2$; (f) EtOH, Na$_2$S$_2$O$_5$, reflux 24 h, (70%).
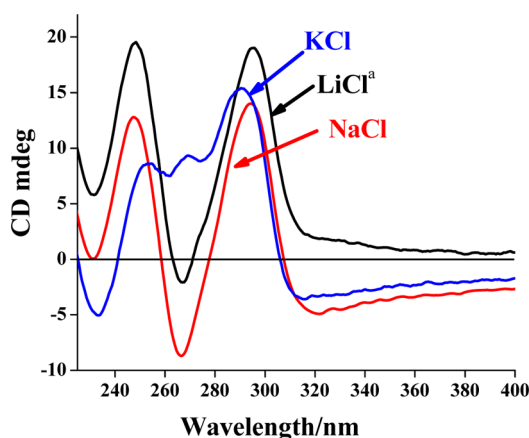

Figure 2. Circular dichroic spectra due to the G4DNA formed by the human telomeric sequence Hum$_{21}$ (4 μM strand concentration) in the presence of indicated ions (100 mM). Superscript "a" indicates having 100 mM Li$^+$ and 10 mM Na$^+$.

telomere DNA in K$^+$ solution.[35,36] For the CD spectra of the G4DNA structures formed in LiCl + Na$^+$ solution, the positions of the peaks matched those of the Na$^+$ stabilized G-quadruplex DNA. However, for the former the positive peaks at 295 and 245 nm were more intense while the negative peak at 264 nm was less intense than those of the latter (Figure 2).

Next we prepared the G4DNA from Hum$_{21}$ sequence in 100 mM LiCl solution. CD spectra of the G4DNA recorded in Li$^+$ solution showed a hump near 277 nm and a peak near 257 nm (Figure S4, Supporting Information). This CD spectral profile is different from that recorded in Li$^+$ +Na$^+$ solution, indicating that topology of the G4DNA is different in Li$^+$ solution.

Next we performed the CD titrations of each Tröger's base ligand with the Hum$_{21}$ G4DNA formed in LiCl + Na$^+$ buffer. No structural change was observed according to the CD spectral profile (Figure 3A and Figure 3B), but the positive peaks at 250 and 295 nm became highly intense showing strong interactions prevailing between each of the ligands **TBBz1** and **TBBz2** with the G4DNA.

CD titrations of the preformed G4DNA formed in 100 mM LiCl solution with the ligands **TBBz1** and **TBBz2** did not show any topology change. The interactions of ligands with DNA were quite strong in this case, and the CD spectra became
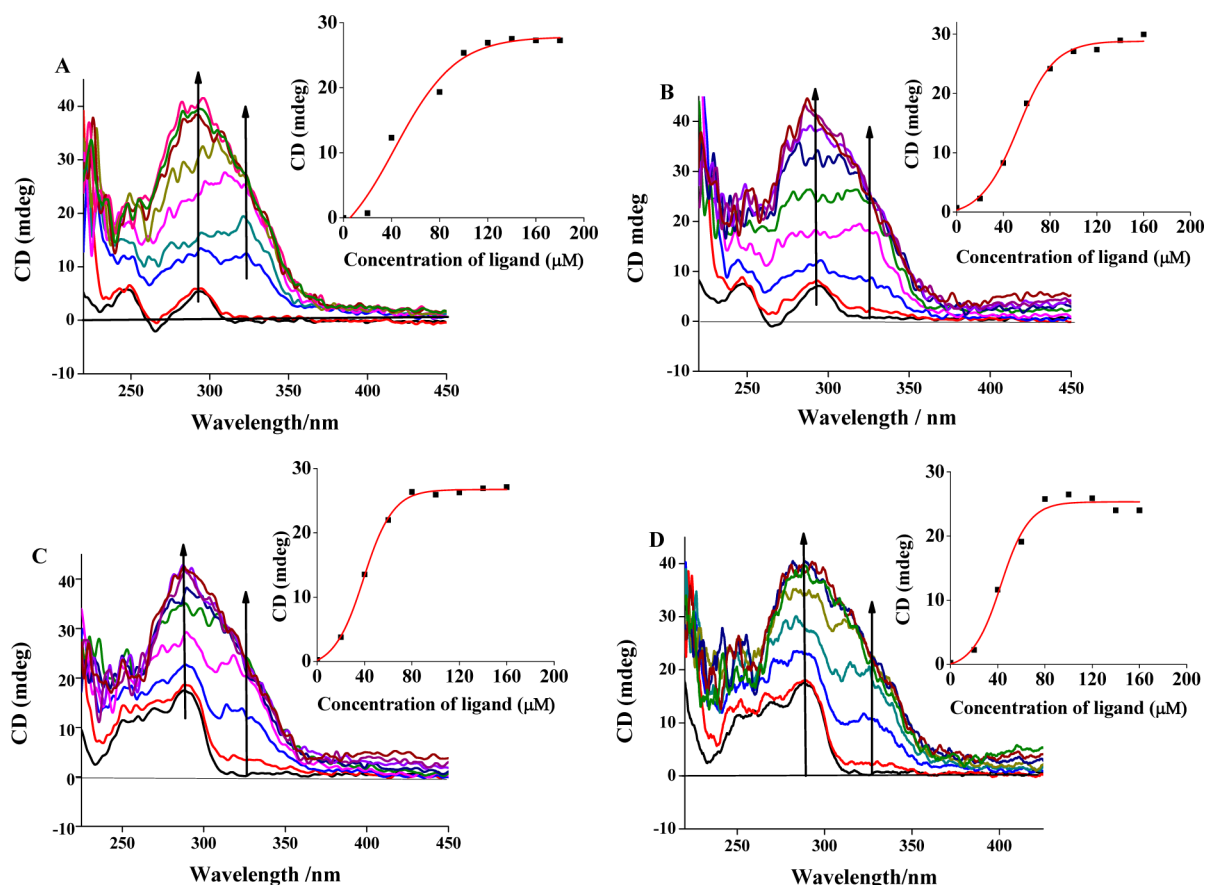
Figure 3. CD spectral titrations of the preformed Hum_{21} G4DNA (4 μM) with **TBBz1** and **TBBz2**: (A, B) in LiCl + Na$^+$ buffer (100 mM LiCl, 10 mM sodium cacodylate, and 0.1 mM EDTA, pH 7.4) and (C, D) in KCl buffer (10 mM Tris-HCl having 100 mM KCl and 0.1 mM EDTA, pH 7.4) with increasing concentration of ligands (0, 20, 40, 60, 80, 100, 120, 140, and 160 μM). Inset shows the increment of ICD band with increasing concentrations of ligand.

distorted after an interaction with 15 equiv of the ligand (Figure S4, Supporting Information).

Solution structure of the K$^+$-stabilized G4DNA has more biological relevance. We therefore performed CD titrations of the preformed G-quadruplex in K$^+$ solution with **TBBz1** and **TBBz2**. The peaks at 245, 270, and 294 nm were intense, and the shallow feature around 232 nm started lifting at lower concentrations of **TBBz1** and **TBBz2** (Figure 3C and Figure 3D). But the conformation of the G4DNA appeared to be the same. Besides the G-quartet planes, the G-quadruplexes also possess several grooves for interaction with a guest molecule.[47] Absence of any isodichoric point in the CD titrations may be due to the presence of more than one G-quadruplex conformation in the solution. This is evident from the NMR spectrum of the 22-mer human telomeric sequence in KCl solution, which had a broad envelope with some fine lines, implying the presence of multiple conformational isomers.[34] An induced CD signal (ICD) appeared near 330 nm after the [ligand]/[DNA] ratio (r) of 10. We say this is ICD because its CD spectral peak intensity is much higher than that of the ligand (without DNA) alone at the same concentration (Figure 3). This ICD signal may appear because of the specific interaction of the ligand with the chiral grooves of the G4DNA. The side chains of the G4DNA binding compounds are also known to have their role in the groove binding.[48]

But dramatic changes occurred in the CD spectral profile of the G4DNA formed in the presence of **TBBz1** and **TBBz2** in

100 mM K$^+$ solution. At ratio "r" of 10, the small positive peak at 245 nm disappeared with concomitant appearance of a shoulder, and a small peak at 270 nm became more intense, while the peak at 295 nm also disappeared (Figure 4). The shallow feature at 232 nm was also red-shifted to 240 nm. Interestingly, at ratio "r" of 10, all three peaks merged to give a
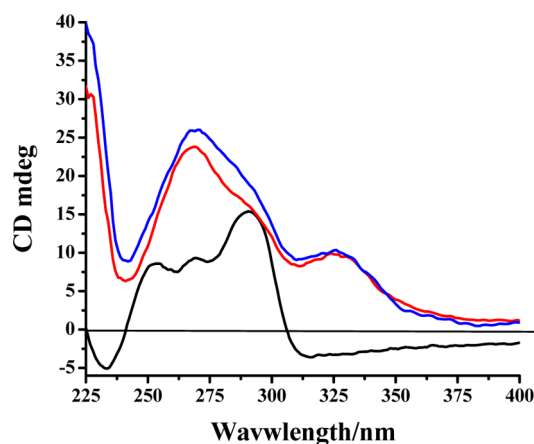
Figure 4. CD spectral profiles of the Hum_{21} (4 μM strand concentration), the G4DNA formed in the presence of **TBBz1** (40 μM) (red) and **TBBz2** (40 μM) (blue) (heated at 90 °C for 5 min and then cooled slowly) in 100 mM KCl buffer (10 mM Tris-HCl having 100 mM KCl and 0.1 mM EDTA, pH 7.4).

peak at 266 nm. This profile is similar to the CD spectral profile of the parallel G4DNAs formed by a number of human and nonhuman telomeric sequences.[28,30,46,49,50]

These results suggest that both **TBBz1** and **TBBz2** are capable of interacting with the preformed G4DNA in K^+ solution without causing any structural alteration. But the ligands are capable of directing the folding of the randomly structured Hum$_{21}$ sequence into the parallel-stranded G4DNA at low concentrations when the G-quadruplex is formed in 100 mM K^+ solution in the presence of the ligands.

In thermal denaturation experiments, **TBBz1** and **TBBz2** showed a characteristic melting curve at 295 nm and provided significant stabilization (9.3 and 9.5 °C respectively) to the preformed Hum$_{21}$ G4DNA in 100 mM LiCl + 10 mM Na^+ solution at [ligand]/[DNA] ratio "r" of 5 (Table 1). We have

Table 1. Melting Temperatures (CD Melting) of the Hum$_{21}$ G4DNA (4 μM Strand Concentration) Formed in LiCl−Na Buffer (100 mM LiCl, 10 mM Sodium Cacodylate, and 0.1 mM EDTA) and the G4DNA Complexed with 10 μM ([ligand]/[DNA] Ratio "r" = 5) of Indicated Compound at 295 nm

entry	ODN/ODN ligand	T_m (°C)	ΔT_m (°C)
1	Hum$_{21}$	37.5	
2	Hum$_{21}$ + **TBBz1**[a]	46.8	9.3
3	Hum$_{21}$ + **TBBz2**[a]	47	9.5

[a]ΔT_m values were obtained from the difference in melting temperatures of the ligand bound and uncomplexed G-quadruplex DNA. The results are the average of two experiments and are within ±0.5 °C of each other.

chosen LiCl + sodium cacodylate solution because Li^+ helps in the formation of G4DNA but Li^+ has insignificant effect on the stability of the G4DNA, and thus, we can have a better idea about the stabilization provided by any G4DNA interacting ligand.[45]

In 100 mM Na^+ solution, the Hum$_{21}$ G4DNA has higher melting temperature (57 °C, Table 2) because of the

Table 2. Melting Temperatures (CD Melting) of the Hum$_{21}$ G4DNA (2 μM Strand Concentration) Formed in NaCl Buffer (10 mM Tris-HCl Having 100 mM NaCl and 0.1 mM EDTA) and the G4DNA Complexed with 20 μM ([Ligand]/[DNA] Ratio "r" = 10) of Indicated Compounds at 295 nm

entry	ODN/ODN ligand	T_m (°C)	ΔT_m (°C)
1	Hum$_{21}$	57	
2	Hum$_{21}$ + **TBBz1**[a]	66	9
3	Hum$_{21}$ + **TBBz2**[a]	68	11

[a]ΔT_m values were obtained from the difference in melting temperatures of the ligand bound and uncomplexed G-quadruplex. The results are the average of two experiments and are within ±0.5 °C of each other.

stabilization provided by the Na^+ ions. To see the effect of each Tröger's base compound on the stability of the G-quadruplex in Na^+ solution, we used a higher ratio "r" of 10. Compounds **TBBz1** and **TBBz2** showed a stabilization of 9 and 11 °C, respectively, in Na^+ solution at 295 nm (Figure S5, Supporting Information; Table 2). The CD melting results were more interesting in 100 mM K^+ solution. This is important because the K^+ solution is more biologically relevant

and K^+ ions form very stable G4DNA structures. It is difficult to measure the stabilization provided by a weak stabilizing ligand in K^+ solution. At "r" of 10, each compound **TBBz1** or **TBBz2** provided slightly less but significant stabilization (8 and 10 °C, respectively, Figure S5, Supporting Information; Table 3) with

Table 3. Melting Temperatures (CD Melting) of the Hum$_{21}$ G4DNA (2 μM) Formed in KCl Buffer (10 mM Tris-HCl Having 100 mM KCl and 0.1 mM EDTA) and the G4DNA Complexed with 20 μM ([Ligand]/[DNA] Ratio "r" = 10) of the Indicated Compounds (at 292 nm for the Preformed G4DNA and at 266 nm for the G4DNA Formed in the Presence of Each Ligand)

entry	ODN/ODN ligand	T_m (°C)	ΔT_m (°C)
1	Hum$_{21}$	65	
2	Hum$_{21}$ + **TBBz1**[a]	73	8
3	Hum$_{21}$ + **TBBz2**[a]	75	10
4	Hum$_{21}$ + **TBBz1**[b]	80	15
5	Hum$_{21}$ + **TBBz2**[b]	82	17

[a]ΔT_m values were obtained from the difference in melting temperatures of the ligand bound and uncomplexed G-quadruplex DNA. [b]The G4 DNA was formed in the presence of the ligand in KCl buffer in the presence of indicated compound (first heated to 90 °C for 5 min and then cooled slowly). The results are the average of two experiments and are within ±0.5 °C of each other.

the preformed K^+-stabilized G4DNA. Stabilization was, however, much higher when the G4DNAs were formed in the presence of **TBBz1** or **TBBz2** at "r" of 10 in 100 mM K^+ solution (15 and 17 °C, respectively, Figure S5, Supporting Information; Table 3).

During the cooling event in KCl solution, the Hum$_{21}$ DNA alone did not form any specific DNA structure (Figure S5C, Supporting Information). Cooling of the solution of the Hum$_{21}$ DNA with **TBBz2** resulted in G-quadruplex formation. Ligands might be directing the folding of DNA into the G4DNA.[51] But the hysteresis was there, and hence the cooling curves were not superimposable with the heating curves.

Absorption Spectral Titrations. The UV−vis spectral titrations involving either of the ligands with the preformed G4DNA resulted in hypochromicity, which indicates a specific binding and strong stacking type of interactions of the ligands with the G4DNA.[28] On the other hand, we observed insignificant hypochromicity in the case of the duplex DNA with each of the above ligands (Figure S6, Supporting Information).

The UV−vis titration results were converted into Scatchard plots, and the binding affinity was obtained upon linear fitting. Ligands **TBBz2** and **TBBz1** both bind strongly to the G4DNA, showing an apparent binding affinity (K_A^{App}) of 4.2×10^5 and 1.4×10^5 M^{-1}, respectively, while for the duplex CT DNA, the corresponding (K_A^{App}) values were nearly 10^2 times smaller for both ligands (Table S2, Supporting Information). These two ligands showed insignificant binding with the corresponding telomeric duplex DNA d[5′-G$_3$(T$_2$AG$_3$)$_3$-3′]/[5′-(C$_3$TA$_2$)$_3$C$_3$-3′] as well (Figure S6, Supporting Information).

Electrophoresis. To examine whether any topology change was caused by each of these ligands, we performed the electrophoretic mobility shift assay using the 5′-^{32}P-end-labeled Hum$_{21}$ G4DNA preformed in 100 mM KCl and the G4DNA formed in the presence of either **TBBz2** or **TBBz1** at different [ligand]/[DNA] ratios in 100 mM KCl solution along with a

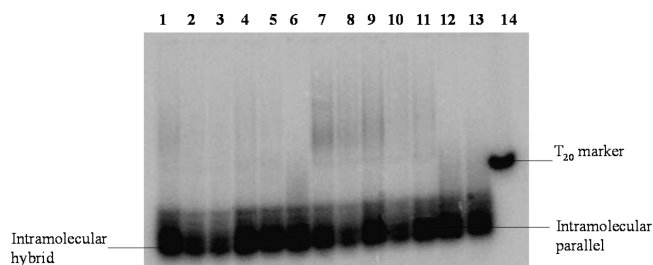dT$_{20}$ marker (control). All the G4DNA bands showed higher mobility than the dT$_{20}$ marker (Figure 5).

Figure 5. Electrophoresis of the G4DNA formed with the Hum$_{21}$ formed in 100 mM KCl. Lane 1: preformed Hum$_{21}$ G4DNA in 100 mM KCl (5 μM). Lane 2: preformed G4DNA in 100 mM KCl + 25 μM **TBBz2**. Lane 3: preformed G4DNA in 100 mM KCl + 25 μM **TBBz1**. Lanes 4−8: 5 μM quadruplex + 15, 25, 40, 50, and 60 μM **TBBz1**. Lanes 9−13: 5 μM G4DNA + 15, 25, 40, 50, and 60 μM **TBBz2**. Lane14: dT$_{20}$ marker. For Lanes 4−13, G4DNA was formed in the presence of **TBBz1** or **TBBz2** (first heated to 90 °C for 5 min and then cooled slowly in 100 mM KCl).

The preformed G4DNA complexed with **TBBz1** or **TBBz2** displayed a similar mobility with the uncomplexed G4DNA alone. This suggests that there is no change in the topology of the G4DNA induced by either ligand. But the G4DNA formed in the presence of **TBBz2** has lower mobility than the preformed G4DNA but higher mobility than the dT$_{20}$ marker (Figure 5). These results are consistent with our recent work where monomeric and dimeric ligands based on symmetrical bisbenzimidazoles folded the Hum$_{21}$ DNA into a parallel stranded G4DNA under similar conditions.[30]

These results are also consistent with those reported earlier for the G4DNA formed by the Hum$_{21}$,[45] where both the hybrid G4DNA and the parallel G4DNA formed in molecularly crowded conditions generated by PEG in KCl solution had higher mobility than the dT$_{21}$ marker and the parallel G4DNA showed intermediate mobility between the hybrid quadruplex and the dT$_{21}$ marker. Hence we believe that the mobility shift in the case of the G4DNA formed in the presence of **TBBz2** was due to the structural conversion and not due to any aggregation, because if it were aggregation, the mobility of the ligand−DNA complex would have been much lower than that of the dT$_{20}$ marker.
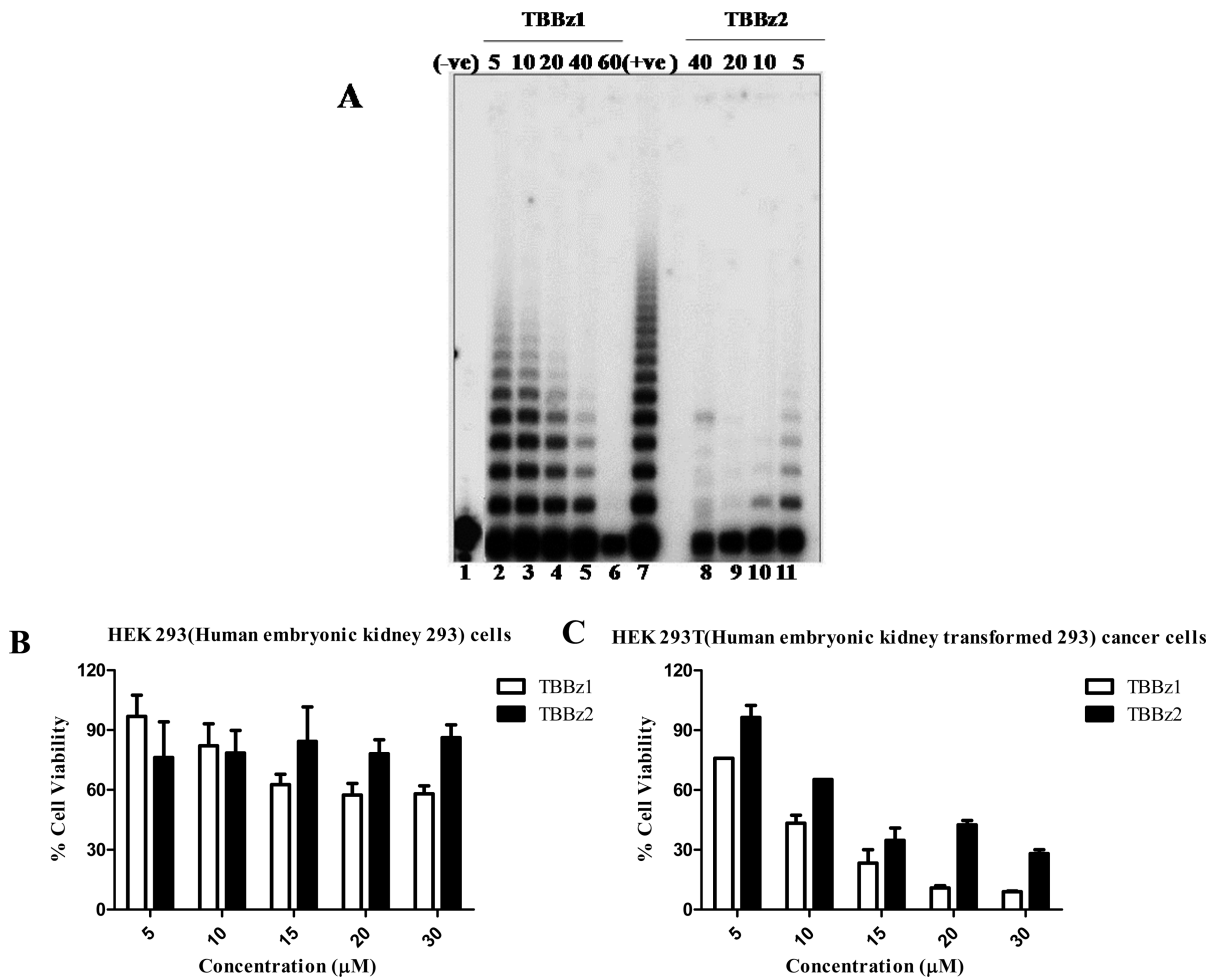

Figure 6. (A) Representative experiments for the determination of telomerase inhibitory properties by the Tröger's base based bisbenzimidazole derivatives. TRAP-LIG assay was performed with increasing concentrations of **TBBz1** and **TBBz2**. Lane 1: (−) ve control (absence of enzyme and ligand). Lanes 2−6: TRAP reaction mixture + 5, 10, 20, 40, and 60 μM **TBBz1**. Lanes 8−11: TRAP reaction mixture + 40, 20, 10, and 5 μM of **TBBz2**. Lane 7: (+) ve control (absence of ligand). (B, C) Effect of the ligands on the cell viability after 48 h of exposure of HEK293 (normal) and HEK293T (cancerous) cells with indicated ligands at various concentrations as measured by MTT (methylthiazolyltetrazolium) assay. Each experiment was performed six times at each point.

Taken together, the CD spectral and the electrophoresis data illustrate that **TBBz2** is capable of directing the folding of the $d[G_3(T_2AG_3)_3]$ into parallel fashion when the G4DNA is formed with the ligands in K^+ solution. The pharmacophore unit of the compounds might be tightly bound at each binding site to provide higher stabilization.

Telomerase Inhibition (TRAP Assay). Telomerase inhibition efficiency of the ligand was measured by a TRAP assay. The G-quadruplex binding agents have been shown to inhibit the telomerase activity through the stabilization of the G-quadruplex structure. This type of ligand acts via a dual role as inhibitors of telomere uncapping and telomerase inhibitors.[52,53] The ligands **TBBz1** and **TBBz2** were evaluated for their ability to inhibit human telomerase using conventional two-step telomerase repeat amplification protocol (TRAP) assay[30] and modified three-step TRAP-LIG protocol assay.[54] In the modified TRAP-LIG assay, we can remove bound and unbound ligands before the PCR amplification assay (see Materials and Methods). Sometimes the ligand has its own inhibitory activity on Taq polymerase, and therefore, it may affect the PCR amplification. Each ligand was tested with increasing concentrations (ranging from 5 to 60 μM) against telomerase extract from A549 (human lung carcinoma cell line) cells. In both cases the ligand **TBBz2** was found to be more potent. In the case of the TRAP-LIG assay protocol, it inhibited the telomerase activity completely at 40 μM (Figure 6A, Figure S7, Supporting Information). Interestingly, **TBBz1** also started inhibiting the telomerase activity at 40 μM and showed full inhibition at 60 μM. The IC_{50} values for the telomerase inhibition by the TRAP-LIG protocol have also been estimated and are shown in Table 4 and in Figure S8, Supporting Information. Importantly, the ligand **TBBz2** displays significantly lower IC_{50} values (at 14.5 μM) than **TBBz1**.

Table 4. IC_{50} against the Telomerase Obtained for Two Ligands by TRAP-LIG Assay[a]

entry	ligand	IC_{50} (μM)
1	**TBBz1**	34.7
2	**TBBz2**	14.5

[a]The results are the average of three experiments and are within $\pm$1% of each other.

Cytotoxicity Assay. To examine the effects of each ligand on three different cancer cell lines HeLa (human cervical cancer transformed cells), A549 (human lung carcinoma transformed cells), and NIH3T3 (mouse embryonic fibroblast cells), short-term cell viability was first determined for 6 and 48 h long cytotoxicity assays (MTT assays) (Figure S9, Supporting Information). Both ligands showed a potent inhibitory effect, and the **TBBz1** was found to be more cytotoxic even at the low concentration.

To evaluate the long-term effects of ligands on these cancer cells, subcytotoxic concentrations (4 μM) of each ligand were employed to avoid acute cytotoxicity and other nonspecific events that could lead to difficulty in the interpretation of results. Generally each ligand was found to have a significantly pronounced inhibitory effect with the three cell lines, but it was observed that **TBBz1** is particularly highly cytotoxic and it was killing 100% of the cancer cell lines at very low concentration (Figure S10, Supporting Information).

To find out the selectivity of the ligands on cancerous vs noncancerous cells, we performed MTT assay on HEK293

(human embryonic kidney 293) normal cells and HEK293T (human embryonic kidney 293 transformed) cancer cells. Both of the ligands were found to be significantly more toxic toward the cancerous cells than the noncancerous cells at all the concentrations used (Figure 6). Interestingly **TBBz1** was found to be more toxic while **TBBz2** was more selective toward the cancer cell. High toxicity of the ligands for the cancer cells over the normal cells may be due to longer telomeres in the cancer cells, which may be folded into the G4DNA, to suppress the activity of overexpressed telomerase.[1−4,12−14]

Computational Studies. It is known that the Tröger's base contains two chiral nitrogen centers. A preliminary molecular modeling study suggested that the nature of binding of such ligands to DNA should be diastereoselective. Since the molecules are chiral, we constructed both enantiomers (R,R)-**TBBz2** and (S,S)-**TBBz2** using GaussView (Figure 7). The geometries were optimized using B3LYP/6-31G* level of theory using Gaussian 03.[55]

To gain further insights into the binding of each ligand with the telomeric G4DNA, an approach that combined molecular docking and MD simulations was adopted. The parallel propeller-type G4DNA structure as reported on the basis of single-crystal X-ray diffraction (PDB 1KF1)[56] was used as the template for the modeling studies. This propeller shaped G4DNA structure could be characterized by two external square planar arrangements found in a simple G4DNA, with base pairing through their Hoogsteen edges. The local G-quartet rise is 3.13 Å with an average 30° right-handed twist between successive ones. The 5′-G-quartet planar surface is relatively more hydrophobic for favoring $\pi-\pi$ stacking interactions, whereas the 3′-G-quartet surface is more favored for electrostatic interactions and both the 5′- and 3′-ends are potential binding sites for each ligand. There are four equivalent phosphate grooves created by the three TTA loops on the side, and these are quite deep and easily accessible for the ligand.[57]

Molecular docking studies were first carried out to predict the possible interactions between the ligands and the G4DNA. It has been previously shown that two types of binding modes are mainly possible for the ligands, and either ligand will stack on the top of the terminal G-tetrads[57,58] with the suggestion that it is energetically unfavorable for them to intercalate between the successive G-tetrads in a G4DNA structure.[59] Ligands can bind to the groove of the G4DNA.[15−19] Therefore, two different docking actions were performed using (R,R)-**TBBz2** with the G-quadruplex DNA (1KF1) and using (S,S)-**TBBz2** with the G4DNA (1KF1). Results from the docking studies suggested that besides having end-stacking interactions, flexible ligands used could be readily accommodated in the groove regions of its propeller-type structures. From the docking study it has been observed that the binding interaction energies of these two enantiomers with G4DNA are almost equal (Table S3).

On the basis of the docking results, we have taken the final docked, lowest energy ligand−G4DNA complexes and then MD simulations (8 ns) were performed on the two complexes formed by the G4DNA (propeller-type) with ligands (R,R)-**TBBz2** and (S,S)-**TBBz2**. All the models were quite stable during the dynamics runs (rmsd values, Figure S13, Supporting Information).

Enantiomer (S,S)-**TBBz2** was found to give two modes of binding. One side of Tröger's base moiety effectively binds over the guanine tetrads and maximizes the stack on the 5′-side of
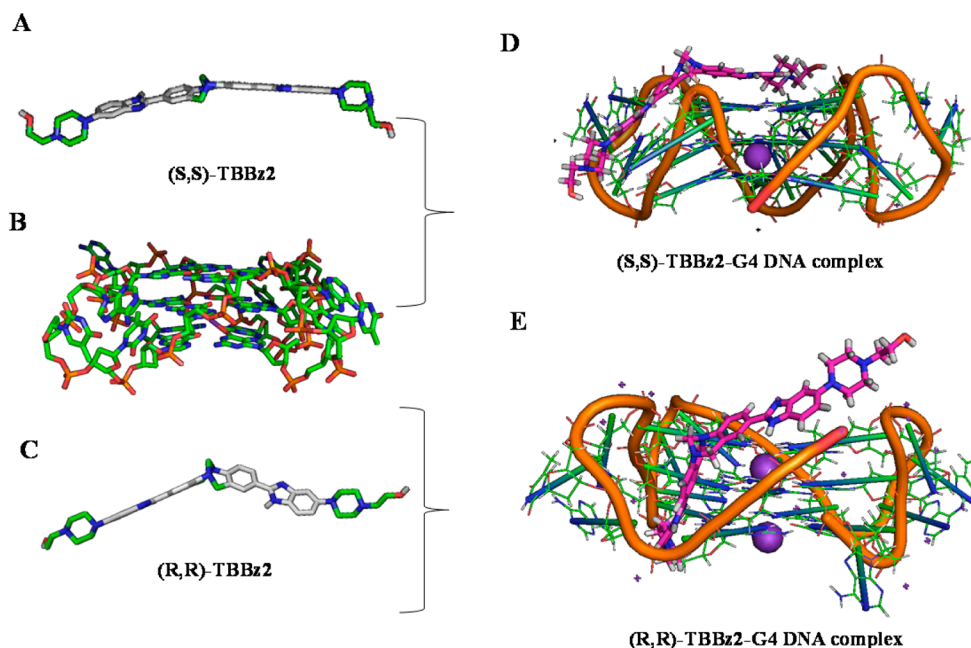
Figure 7. Optimized structures at the B3LYP/6-31G* level of theory of (A) (*S*,*S*)-**TBBz2** and (C) (*R*,*R*)-**TBBz2**. (B) Structures of the G-tetrad: model of ligand−G4DNA complex. (D, E) One-half of (*S*,*S*)-**TBBz2** is stacking on the surface of G-quartet, while other half is involved in groove binding (D) and (*R*,*R*)-**TBBz2** binding to the loop of G4DNA (E).

the π−π face. Because of the easily accessible groove of the G4DNA, the other side of this enantiomer was fitting itself into the groove created by the TTA loops, which is consistent with the occurrence of ICD signals in the CD spectra. The rigid concave shaped Tröger's base scaffold was found to bind on the TTA loop and interact with the phosphate backbone as well (Figure 7 and Figure S11). During the simulation it has been observed that one K$^+$ ion comes from the bulk solution and is placed between the adjacent G-tetrad planes and stabilizes the whole complex. Hence, the molecular organization of the central core (internal H-bonds) and the electronic/electrostatic properties make these compounds almost perfectly suitable to recognize G4DNA.

The other enantiomer (*R*,*R*)-**TBBz2** possessed much more favorable groove binding interactions with the parallel-propeller G4DNA. The (*R*,*R*)-enantiomers generally form the right-handed helical twist, and thus, it is easily accumulating itself to the right-handed twisted grooves of the G4DNA (Figure 7 and Figure S12).

CONCLUSIONS

Herein we have designed and synthesized two novel bisbenzimidazole substituted Tröger's base ligands that provide pronounced stabilization of the G4DNA assembled from a human telomere sequence. This occurs in both cases, with the preformed G4DNA and the G4DNA formed in presence of the ligands. The ligands are capable of directing the folding of the telomeric DNA into an unusually stable parallel-stranded conformation (as evident from the CD melting and electrophoresis data) when the G4DNA is formed along with the ligand in K$^+$ solution. Binding constant data obtained from the absorption titrations suggest much lower affinity of the ligands toward the duplex DNA compared to that of the G4DNA. Both of the ligands showed significant trends of inhibitory effect against telomerase activity. Long-term cell proliferation studies at subcytotoxic concentrations with the ligands using different

cancer cell lines have suggested that the ligands produce high order growth arrest of the cancer cells and at the same time these molecules were more selective toward the cancer cells rather than the corresponding normal cells. Molecular modeling studies suggest that the mode of binding of the ligand molecules on the G4DNA is influenced by the helical twist of the ligand. The present study clearly suggests that these types of molecules having rigid Tröger's base tweezer-like skeletons might offer themselves as potential lead compounds for the development of a new class of anticancer drugs.

MATERIALS AND METHODS

Materials. All starting materials were from the best known commercial sources and used as received. All solvents were from Merck, and they were distilled and/or dried prior to use whenever necessary. All tested ligands were found to be at least >95% pure by elemental analysis (Table S1, Supporting Information).

General Spectrometric Characterization. ^{1}H (300 or 400 MHz) and ^{13}C NMR (75 or 100 MHz) spectra were recorded on a Bruker AMX spectrometer. IR spectra were recorded on an FT-IR Perkin-Elmer Spectrum GX spectrometer. Melting points were taken on open capillaries inside a Buchi melting point B540 apparatus and are uncorrected. Mass spectra were recorded on a Micromass Q-TOF Micro spectrometer. MALDI mass spectra were recorded on an Ultraflex TOF/TOF mass spectrometer (Bruker Daltonics, Bremen, Germany) in positive ion mode, using α-cyano-4-hydroxylcinnamic acid as a matrix.

6H,12H-5,11-Methanodibenzo[*b*,*f*][1,5]diazocine-2,8-dicarboxylic Acid Diethyl Ester (1). A mixture of *p*-aminoethyl benzoate (1 g, 6.6 mmol) and paraformaldehyde (331 mg) in trifluoroacetic acid (TFA) (25 mL) was stirred at room temperature. After 72 h, TFA was removed by distillation. The residue was taken in 60 mL of water, poured into a separatory funnel, and basified by the addition of concentrated NH$_4$OH. The aqueous layer was then extracted with EtOAc (100 mL). The combined organic phases were collected, dried over Na$_2$SO$_4$, filtered, and concentrated in vacuo to give the crude product as a yellow glass foam. The crude product was purified by column chromatography using EtOAc in *n*-hexane (10%) as the eluent to give the required compound **2** as a yellow crystalline solid. Yield:

288 mg, 42%. Mp: 127−128 °C (reported 126−129 °C).[21] IR: 3362.28, 2981.41, 2907.16, 1702.84, 1590.02, 1416.46, 1279.76 cm^{-1}. ^{1}H NMR (CDCl$_3$) δ 8.1 (d, 2H, J = 5.5 Hz), 7.9 (d, 2H, J = 5.0 Hz), 7.7 (d, 2H, J = 3.7 Hz), 5.0 (s, 2H), 4.2 to 4.4 (m, 8H), 1.3, (t, 6H, J = 5 Hz). m/z (Q-TOF HRMS) found, 367.1612 (calcd, 367.1590, [M + H]$^+$).

(8-Hydroxymethyl-6*H*,12*H*-5,11-methanodibenzo[*b*,*f*][1,5]-diazocin-2-yl)methanol (2). Compound **2** (0.6 g, 1.75 mmol) was dissolved in dry THF (15 mL), and lithium aluminum hydride (400 mg, 9.0 mmol) was added under ice-cold conditions. The reaction mixture was allowed to come to room temperature and stirred for 12 h, after which the reaction was quenched with aqueous solution of Na−K tartrate and the compound was extracted with 10% MeOH in CHCl$_3$. The organic layer was dried over anhydrous Na$_2$SO$_4$, and then the solvents were removed under vacuum. The crude product was purified with column chromatography using neutral alumina. The required compound was eluted out with 5−8% MeOH in CHCl$_3$ to obtain a white gummy solid in 65% yield (110 mg). IR: 3353.8, 2955.41, 2925.77, 1494.19, 1463.4, 1377.55, 1216.83, 1045.99 cm^{-1}. ^{1}H NMR (CDCl$_3$) δ 7.2 (bs, 2H), 7.0 (bs, 2H), 6.7 (bs, 2H), 4.5 (s, 2H), 4.0 (bs, 4H). m/z (Q-TOF HRMS) found, 283.3448 (calcd, 283.3450, [M + H]$^+$).

6*H*,12*H*-5,11-Methanodibenzo[*b*,*f*][1,5]diazocine-2,8-dicar-baldehyde (3). To a stirred suspension of compound **3** (0.8 g, 2.8 mmol) in dry THF (15 mL) was added pyridinium chlorochromate (3 equiv) along with 1.2 g of silica. Stirring was continued at room temperature for 12 h. Once TLC showed the disappearance of the diol derivative, the solvent was removed and the crude solid was adsorbed onto neutral alumina (∼7 g). The product was eluted out with 2−3% MeOH in chloroform through an open column. The product isolated was a gummy solid (68% yield, 529 mg) and used for the subsequent step without further purification. IR: 3356.82, 2950.47, 2929.77, 1680.34, 1490.20, 1465.4, 1218.83 cm^{-1}. ^{1}H NMR (CDCl$_3$) δ 9.7 (s, 2H), 8.46 (d, 2H, J = 5.3 Hz), 7.75 (d, 2H, J = 5.0 Hz), 6.7 (d, 2H, J = 4.25 Hz), 4.4 (s, 2H), 4.1 (m, 4H). m/z (Q-TOF HRMS) found, 279.3134 (calcd, 279.3132, [M + H]$^+$).

(±)-2,8-Bis-[6-(4-methylpiperazin-1-yl)-1*H*-benzoimidazol-2-yl]-6*H*,12*H*-5,11-methanodibenzo[*b*,*f*][1,5]diazocine (±)-TBBz1). To a freshly prepared solution of 4-(4-methylpiperazin-1-yl)benzene-1, 2-diamine (**6**, 103 mg, 0.5 mmol)[28] was added dialdehyde (**3**, 69.5 mg, 0.25 mmol). To this solution was added sodium metabisulfite (Na$_2$S$_2$O$_5$, 2 equiv dissolved in minimum quantity of water). The reaction mixture was refluxed for 12 h with stirring, then cooled to room temperature, and filtered through Celite. Solvent from the filtrate was then removed under reduced pressure to obtain a crude product. This product was then purified using column chromatography (a gradient of EtOAc/MeOH) on silica gel (70−220 mesh size) to obtain the required product as a brown hygroscopic solid. Yield: 214.6 mg, 66%. Mp: >290 °C. IR: 3408.5, 3016, 2878.6, 1616, 1565, 1450.5, 1221 cm^{-1}. ^{1}H NMR (DMSO-d_6) δ 11.1 (bs, 2H), 7.9 (d, 2H, J = 5.2 Hz), 7.5 (bs, 2H), 6.9−7.2 (m, 6H), 6.8 (d, 2H, J = 5.4 Hz), 4.22 (s, 2H), 3.85 (bs, 4H), 3.1 (bs, 8H), 2.2−2.5 (bs, 14H). ^{13}C NMR (DMSO-d_6) δ 154.61, 149.62, 139.50,135.80, 130.01, 128.52, 124.52, 117.82, 115.52, 112.46, 107.43, 101.70, 67.20, 55.03, 54.90,54.80, 51.5, 43.75. m/z (MALDI-TOF) found, 651.351 (calcd, 651.359, [M + H]$^+$). Anal. Calcd for C$_{39}$H$_{42}$N$_{10}$·H$_2$O: C, 71.75; H, 6.79; N, 21.46. Found: C, 71.72; H, 6.81; N, 21.42.

(±)-2-{4-[2-(8-{6-[4-(2-Hydroxyethyl)piperazin-1-yl]-1*H*-benzoimidazol-2-yl}-6*H*,12H-5,11-methanodibenzo[*b*,*f*][1,5]-diazocin-2-yl)-3*H*-benzoimidazol-5-yl]piperazin-1-yl}ethanol (±TBBz2). To a freshly prepared solution of 4-[4-(2-hydroxyethyl)-piperazin-1-yl]benzene-1,2-diamine (**7**, 118 mg, 0.5 mmol)[2] was added dialdehyde (**3**, 69.5 mg, 0.25 mmol). To this solution was added sodium metabisulphite (Na$_2$S$_2$O$_5$, 2 equiv dissolved in minimum quantity of water) was added. The reaction mixture was refluxed for 12 h with stirring, then cooled to room temperature, and filtered through Celite. Solvent from the filtrate was then removed under reduced pressure to obtain a crude product. This crude product is then purified by column chromatography (a gradient of EtOAc/MeOH) on silica gel (70−220 mesh size) to obtain the required product as a brown

hygroscopic solid. Yield: 224 mg, 63%. Mp: > 290 °C. IR: 3410, 3016, 2878, 1614, 1565, 1450, 1220 cm^{-1}. ^{1}H NMR (DMSO-d_6) δ 11.0 (bs, 2H), 8.2 (m, 2H), 7.8 (d, 2H, J = 5.4 Hz), 6.9−7.4 (m, 6H), 6.7 (d, 2H, J = 5.3 Hz), 6.1 (s, 2H), 4.2 (s, 2H), 3.9 (s, 4H), 3.6 (bs, 12H), 2.4−2.6 (bs, 12H). ^{13}C NMR (DMSO-d_6) δ 161.12, 148.93, 139.40, 134.80, 129.16, 128.33, 121.18, 116.65, 115.73, 112.0, 106.93, 102.56, 67.20, 60.36, 57.94, 54.12, 51.24, 44.83. m/z (MALDI-TOF) found, 711.469 (calcd, 711.382, [M + H]$^+$). Anal. Calcd for C$_{41}$H$_{46}$N$_{10}$·1.5H$_2$O: C, 66.74; H, 6.69; N, 18.98. Found: C, 66.70; H, 6.71; N, 18.93.

Resolution of TBBz1 and TBBz2 Using Dibenzoyl-(+)-tartaric Acid.[42] The dibenzoyl-(+)-tartaric acid (2.2 equiv) and racemic mixture of each Tröger's base derivative, (±)-TBBz 1 or (±)-TBBz2 (1 equiv), were taken in MeOH/CHCl$_3$ (3:1) (15 mL) and the contents stirred at 25 °C for 12 h. The precipitate was collected and suspended in a mixture of 1-butanol (20 mL) and 2 M Na$_2$CO$_3$ and stirred until dissolution occurred. The organic layer was separated and the aqueous layer extracted with 1-butanol (2 × 15 mL). The combined organic extracts were washed with brine (10 mL) anddried over anhydrous Na$_2$SO$_4$. Solvent was then removed under reduced pressure to obtain a solid product. With this solid product we measured the circular dichroic spectra and we obtained some enrichment of the (+)-enantiomer. The filtrate was concentrated carefully at 10 °C, and with the residue we measured CD spectra which confirmed the enrichment of the (+)-enantiomer.

Oligonucleotides. HPLC purified oligodeoxyribonucleotides (ODN) d[G$_3$(T$_2$AG$_3$)$_3$], abbreviated as Hum$_{21}$, and dT$_{20}$ were purchased from Sigma Genosys, Bangalore, India. Their purity was confirmed using high resolution sequencing gel. The molar concentration of each ODN was determined from absorbance measurements at 260 nm based on their molar extinction coefficients (ε_{260}) of 215 000 and 148 400 for d[G$_3$(T$_2$AG$_3$)$_3$] and dT$_{20}$, respectively.

G4DNA Formation. Single-stranded d[G$_3$(T$_2$AG$_3$)$_3$] was dissolved in an appropriate buffer at the indicated concentration. The solution was first heated at 90 °C for 5 min and then cooled slowly to room temperature over a period of 24 h.

Circular Dichroism Spectroscopy, T_m Studies, Absorption Titrations, Polyacrylamide Gel Electrophoresis, Telomerase Assay, and Computational Methods. These experiments were performed as described in our earlier reports.[28−31]

TRAP-LIG Assay.[54] The TRAP assay was performed using a three-step TRAP-LIG procedure: (i) primer elongation by telomerase and addition of ligand, (ii) subsequent removal of the ligand, and (iii) PCR amplification of the products of telomerase elongation.

Step 1. This was carried out by preparing a master mix containing 0.1 μg of TS forward primer (5′-AAT CCG TCG AGC AGA GTT-3′), TRAP buffer (20 mM Tris-HCl, pH 8.3, 68 mM KCl, 1.5 mM MgCl$_2$, 1 mM EGTA, and 0.05% [v/v] Tween 20), dNTPs (125 μM each), and protein extract (500 ng/sample) diluted in lysis buffer (10 mM Tris-HCl, pH 7.5, 1 mM MgCl$_2$, 1 mM EGTA, 0.5% CHAPS, 10% glycerol, 5 mM β-mercaptoethanol, and 0.1 mM 4-(2-aminoethyl)benzenesulfonyl fluoride. The PCR master mix was added to tubes containing freshly prepared ligand at various concentrations and to a negative control containing no ligand. The initial elongation step was first out carried at 30 °C for 10 min, then at by 94 °C for 5 min and finally maintaining the mixture at 20 °C.

Step 2. To purify the elongated product and to remove the bound ligands, the QIA quick nucleotide purification kit (Qiagen) was used according to the manufacturer's instructions. This kit is specially designed for the purification of both double- and single-stranded ODNs from 17 bases in length. It employs a high-salt buffer to bind the negatively charged ODNs to the positively charged spin tube membrane through centrifugation so that all other components, including positively charged and neutral ligand molecules, are eluted. PCR-grade water was then used (rather than the manufacturer's recommendation of an ethanol based buffer) to wash any impurities away before elution of the DNA using a low-salt concentration solution. The purified samples were freeze-dried and then redissolved

in PCR-grade water at room temperature prior to the second amplification step.

Step 3. The purified extended samples were then subjected to PCR amplification. For this, a second PCR master mix was prepared consisting of 1 μM ACX reverse primer (5′-GCG CGG [CTTACC]$_3$ CTA ACC-3′), 0.1 μg of TS forward primer (5′-AAT CCG TCG AGC AGA GTT-3′), TRAP buffer, 5 μg of BSA, 0.5 mM dNTPs, and 2 U of Taq polymerase. A 6 μL aliquot of the master mix was added to the purified telomerase extended samples and amplified for 30 cycles of 30 s at 94 °C and 30 s at 59 °C. The reaction products were loaded onto a 10% polyacrylamide gel (19:1) in TBE, 0.5×. Gels were transferred to Whatman 3 mm paper, dried under vacuum at 80 °C, and read using a phosphorimager 840 (Amersham). Measurements were made in triplicate with respect to a negative control run using the equivalent TRAP-PCR conditions but omitting the protein extract, thus ensuring that the ladders observed were not due to artifacts of the PCR reaction.

Short-Term Cell Viability Assay. HeLa (human cervical cancer transformed cells) and A549 (human lung carcinoma transformed cells) and NIH3T3 (mouse embryonic fibroblast cells) cells were seeded in 96-well plates (15.0×10^3/well). Cells were grown for 24 h before treatment to get 70% confluency and exposed to various concentrations of ligands in the presence of 0.2% FBS. After 6 or 48 h of incubation at 37 °C in a humidified atmosphere of 5% CO_2, the old medium was replaced with the new one having 10% FBS containing DMEM, and cells were further grown for 42 h after treatment. Then 20 μL of a 5 mg/mL solution of methylthiazolyltetrazolium (MTT) reagent was added to 200 μL of medium present in each well and cells were further incubated for 4 h. The old medium was discarded. Formazan crystals were dissolved in DMSO, and a reading (fluorescence) was taken at 595 nm in ELISA plate reader. All ligand doses were tested in parallel in triplicate.

Percentage cell viability was calculated using the formula

$$\% \text{ cell viability} = [(\text{FI}_{(595)} \text{ of treated cells}$$
$$- \text{FI}_{(595)} \text{ of plain DMSO})$$
$$/(\text{FI}_{(595)} \text{ of untreated cells}$$
$$- \text{FI}_{(595)} \text{ of plain DMSO})] \times 100$$

Long-Term Cell Culture Experiments. Long-term proliferation experiments were carried out using HeLa, A549, and NIH3T3 cell lines. Cells were grown in six-well tissue culture plates at 5.0×10^4 per well and exposed to a subcytotoxic concentration of 4 μM or an equivalent volume of 0.1% DMSO every 5 days. The cells in control and ligand-exposed wells were counted, and wells were reseeded with half population of cells. This process was continued for 15 days. Cell population versus time (days) graphs were generated.

Selectivity toward Cancerous Cells. HEK293 (human embryonic kidney 293) normal cells and HEK293T ((human embryonic kidney transformed 293) cancer cells were seeded in 96-well plates (8.0×10^3/well). Experiments were performed as in the case of the short-term cell viability assay.

ASSOCIATED CONTENT

⑤ Supporting Information

Characterization results for **TBBz1** and **TBBz2**, ^{1}H and ^{13}C NMR of ligands, additional CD and UV−vis data, computational results, CD melting curves, and additional cytotoxicity data. This material is available free of charge via the Internet at http://pubs.acs.org.

AUTHOR INFORMATION

Corresponding Author
*Phone: (91) 80-22932664. Fax: (91) 80-23600529. E-mail: sb@orgchem.iisc.ernet.in.

ABBREVIATIONS USED
G4DNA, G-quadruplex DNA; ODN, oligodeoxynucleotide; CD, circular dichroism; ICD, induced circular dichorism; PEG, polyethylene glycol; TRAP, telomerase repeat amplification protocol; FI, fluorescence intensity; EDTA, ethylenediaminetetraacetic acid; MTT, methylthiazolyltetrazolium; DMSO, dimethyl sulfoxide; NMR, nuclear magnetic resonance; MALDI, matrix assisted laser desorption ionization; IR, infrared

REFERENCES
(1) Blackburn, E. H. Telomeres: no end in sight. *Cell* **1994**, 77, 621−623.
(2) Jain, A. K.; Bhattacharya, S. Interaction of G-quadruplexes with non-intercalating DNA minor groove binding ligands. *Bioconjugate Chem.* **2011**, 22, 2355−2368.
(3) Greider, C. W. Telomere length regulation. *Annu. Rev. Biochem.* **1996**, 65, 337−365.
(4) Tauchi, T.; Shin-Ya, K.; Sashida, G.; Sumi, M.; Obake, S.; Ohyashiki, J. H.; Ohyashiki, K. Telomerase inhibition with a novel G-quadruplex-interactive agent, telomestatin: in vitro and in vivo studies in acute leukemia. *Oncogene* **2006**, 25, 5719−5725.
(5) Zhou, J.-L.; Lu, Y.-J.; Ou, T.-M.; Zhou, J.-M.; Huang, Z.-S.; Zhu, X.-F.; Du, C.-J.; Bu, X.-Z.; Ma, L.; Gu, L.-Q.; Li, Y.-M.; Chan, A. S.-C. Synthesis and evaluation of quindoline derivatives as G-quadruplex inducing and stabilizing ligands and potential inhibitors of telomerase. *J. Med. Chem.* **2005**, 48, 7315−7321.
(6) Mergny, J. L.; Riou, J. F.; Mailliet, P.; Teulade-Fichou, M. P.; Gilson, E. Natural and pharmacological regulation of telomerase. *Nucleic Acids Res.* **2002**, 30, 839−865.
(7) Cian, A. D.; Lacroix, L.; Douarre, C.; Smaali, N. T.; Trentesaux, C.; Riou, J.; Mergny, J. L. Targeting telomeres and telomerase. *Biochimie* **2008**, 90, 131−155.
(8) Rezler, E. M.; Bearss, D. J.; Hurley, L. H. Telomere inhibition and telomere disruption as proceaaes for drug targeting. *Annu. Rev. Pharmacol. Toxicol.* **2003**, 43, 359−379.
(9) Zahler, A. M.; Williamson, J. R.; Cech, T. R.; Prescott, D. M. Inhibition of telomerase by G-quartet DNA formation. *Nature* **1991**, 350, 718−720.
(10) Leonetti, C.; Amodei, S.; D'Angelo, C.; Rizzo, A.; Benassi, B.; Antonelli, A.; Elli, R.; Stevens, M. F. G.; D'Incalci, M.; Zupi, G.; Biroccio, A. Biological activity of the G-quadruplex ligand RHPS4 (3,11-difluoro-6,8,13-trimethyl-8H-quino[4,3,2-kl]acridinium methosulfate) is associated with telomere capping alteration. *Mol. Pharmacol.* **2004**, 66, 1138−1146.
(11) (a) Neidle, S. Human telomeric G-quadruplex: the current status of telomeric G-quadruplexes as therapeutic targets in human cancer. *FEBS J.* **2010**, 277, 1118−1125. (b) Franceschin, M. J. G quadruplex DNA structures and organic chemistry: more than one connection. *Eur. J. Org. Chem.* **2009**, 2225−2238.
(12) Chakraborty, T. K.; Arora, A.; Roy, S.; Kumar, N.; Maiti, S. Furan based cyclic oligopeptides selectively target G-quadruplex. *J. Med. Chem.* **2007**, 50, 5539−5542.
(13) Jain, A. K.; Bhattacharya, S. Recent developments in the chemistry and biology of G quadruplexes with reference to the DNA groove binders. *Curr. Pharm. Des.* **2012**, 18, 1917−1933.

(14) Folini, M.; Venturini, L.; Cimino-Reale, G.; Zaffaroni, N. Telomeres as targets for anticancer therapies. *Expert Opin. Ther. Targets* **2011**, *15*, 579−593.

(15) Kerwin, S. M. G-Quadruplex DNA as a target for drug design. *Curr. Pharm. Des.* **2000**, *6*, 441−478.

(16) Randazzo, A.; Galeone, A.; Esposito, V.; Varra, M.; Mayol, L. Interaction of distamycin A and netropsin with quadruplex and duplex structures: a comparative 1H-NMR study. *Nucleosides, Nucleotides Nucleic Acids* **2002**, *21*, 535−545.

(17) Randazzo, A.; Galeone, A.; Mayol, L. ¹H-NMR study of the interaction of distamycin A and netropsin with the parallel stranded tetraplex [d(TGGGGT)]₄. *Chem. Commun.* **2001**, *11*, 1030−1031.

(18) (a) Chaudhuri, P.; Ganguly, B.; Bhattacharya, S. An experimental and computational analysis on the differential role of the positional isomers of symmetric bis-2-(pyridyl)-1H-benzimidazoles as DNA binding agents. *J. Org. Chem.* **2007**, *72*, 1912−1923. (b) Chaudhuri, P.; Majumder, H. K.; Bhattacharya, S. Synthesis, DNA binding, and Leishmania topoisomerase inhibition activities of a novel series of anthra[1,2-d]imidazole-6,11-dione derivatives. *J. Med. Chem.* **2007**, *50*, 2536−2540.

(19) Phan, A. T.; Kuryavyi, V.; Gaw, H. Y.; Patel, D. J. Small-molecule interaction with a five guanine-tract G-quadruplex structure from the human MYC promoter. *Nat. Chem. Biol.* **2005**, *1*, 167−163.

(20) Vögtle, F. *Fascinating Molecules in Organic Chemistry*; Wiley: Chichester, U.K., 1992; pp 237−249.

(21) Goswami, S.; Ghosh, K.; Dasgupta, S. Troger's base molecular scaffolds in dicarboxylic acid recognition. Troger's base molecular scaffolds in dicarboxylic acid recognition. *J. Org. Chem.* **2000**, *65*, 1907−1914.

(22) Thilgen, C.; Gosse, I.; Diederich, F. *Top. Stereochem.* **2003**, *23*, 1−124.

(23) Veale, E. B.; Frimannsson, D. O.; Lawler, M.; Gunnlaugsson, T. 4-Amino-1,8-naphthalimide based Tröger's bases as high affinity DNA targeting fluorescent supramolecular scaffolds. *Org. Lett.* **2009**, *11*, 4040−4043.

(24) Valik, M.; Malina, J.; Palivec, L.; Foltynova, J.; Tkadlecova, M.; Urbanova, M.; Brabecb, V.; Krala, V. Tröger's base scaffold in racemic and chiral fashion as a spacer for bis-distamycin formation. Synthesis and DNA binding study. *Tetrahedron* **2006**, *62*, 8591−8600.

(25) (a) Bailly, C.; Laine, W.; Demeunynck, M.; Lhomme, J. Enantiospecific recognition of DNA sequences by a proflavine Tröger base. *Biochem. Biophys. Res. Commun.* **2000**, *273*, 681−685. (b) Tatibouët, A.; Demeunynck, M.; Andraud, C.; Collet, A.; Lhomme, J. Synthesis and study of an acridine substituted Tröger's base: preferential binding of the (−)-isomer to B-DNA. *Chem. Commun.* **1999**, 161−162.

(26) Johnson, R. A.; Gorman, R. R.; Wnuk, R. J.; Crittenden, N. J; Aiken, J. W. Tröeger's base. An alternate synthesis and a structural analog with thromboxane A2 synthetase inhibitory activity. *J. Med. Chem.* **1993**, *36*, 3202−3206.

(27) Harmata, M.; Kahraman, M. Congeners of Troeger's base as chiral ligands. *Tetrahedron: Asymmetry* **2000**, *11*, 2875−2879.

(28) Jain, A. K.; Reddy, V. V.; Paul, A.; Muniyappa, K.; Bhattacharya, S. Synthesis and evaluation of a novel class of G-quadruplex-stabilizing small molecules based on the 1,3-phenylenebis-(piperazinylbenzimidazole) system. *Biochemistry* **2009**, *48*, 10693−10704.

(29) Bhattacharya, S.; Chaudhuri, P.; Jain, A. K.; Paul, A. Symmetrical bisbenzimidazoles with benzenediyl spacer: the role of the shape of the ligand on the stabilization and structural alterations in telomeric G-quadruplex DNA and telomerase inhibition. *Bioconjugate Chem.* **2010**, *21*, 1148−1159.

(30) Jain, A. K.; Paul, A.; Maji, B.; Muniyappa, K.; Bhattacharya, S. Dimeric 1,3-phenylene-bis(piperazinyl benzimidazole)s: synthesis and structure−activity investigations on their binding with human telomeric G-quadruplex DNA and telomerase inhibition properties. *J. Med. Chem.* **2012**, *55*, 2981−2993.

(31) Paul, A.; Jain, A. K.; Misra, S. K.; Maji, B.; Muniyappa, K.; Bhattacharya, S. Binding of gemini bisbenzimidazole drugs with human

(32) Wang, Y.; Patel, D. J. Solution structure of the human telomeric repeat d[AG₃(T₂AG₃)₃] G-tetraplex. *Structure* **1993**, *1*, 263−282.

(33) Yang., D.; Okamoto, K. Structural insights into G-quadruplexes: towards new anticancer drugs. *Future Med. Chem.* **2010**, *2*, 619−646.

(34) Ambrus, A.; Chen, D.; Dai, J.; Bialis, T.; Jones, R. A.; Yang, D. Human telomeric sequence forms a hybrid-type intramolecular G-quadruplex structure with mixed parallel/antiparallel strands in potassium solution. *Nucleic Acids Res.* **2006**, *34*, 2723−2735.

(35) Xue, Y.; Kan, Z.; Wang, Q.; Yao, Y.; Liu, J.; Hao, Y.; Tan, Z. Human telomeric DNA forms parallel-stranded intramolecular G-quadruplex in K⁺ solution under molecular crowding condition. *J. Am. Chem. Soc.* **2007**, *129*, 11185−11191.

(36) Stokke, T.; Steen, H. B. Multiple binding modes for Hoechst 33258 to DNA. *J. Histochem. Cytochem.* **1985**, *33*, 333−338.

(37) Jain, A. K.; Awasthi, S. K.; Tandon, V. Triple helix stabilization by covalently linked DNA−bisbenzimidazole conjugate synthesized by maleimide−thiol coupling chemistry. *Bioorg. Med. Chem.* **2006**, *14*, 6444−6452.

(38) Bhattacharya, S.; Chaudhuri, P. Medical implications of benzimidazole derivatives as drugs designed for targeting DNA and DNA associated processes. *Curr. Med. Chem.* **2008**, *15*, 1762−1777.

(39) Tawar, U.; Jain, A. K.; Dwarakanath, B. S.; Chandra, R.; Singh, Y.; Chaudhury, N. K.; Khaitan, D.; Tandon, V. Influence of phenyl ring disubstitution on bisbenzimidazole and terbenzimidazole cytotoxicity: synthesis and biological evaluation as radioprotectors. *J. Med. Chem.* **2003**, *46*, 3785−3792.

(40) Paul, A.; Bhattacharya, S. Chemistry and biology of DNA-binding small molecules. *Curr. Sci.* **2012**, *102*, 212−231.

(41) Jain, A. K.; Bhattacharya, S. Groove binding ligands for the interaction with parallel-stranded *ps*-duplex DNA and triplex DNA. *Bioconjugate Chem.* **2010**, *21*, 1389−1403.

(42) Satishkumar, S.; Periasamy, M. A convenient method for the synthesis and resolution of Tröger's base. *Tetrahedron: Asymmetry* **2006**, *17*, 1116−1119.

(43) Turner, J. J.; Harding, M. M. Synthesis and properties of chiral molecular clefts related to Tröger's base. *Supramol. Chem.* **2005**, *17*, 369−375.

(44) Baldeyrou, B.; Tardy, C.; Bailly, C.; Colson, P.; Houssier, C.; Charmantray, F.; Demeunynck, M. Synthesis and DNA interaction of a mixed proflavine−phenanthroline Tröger base. *Eur. J. Med. Chem.* **2002**, *37*, 315−322.

(45) Cian, A.; De.; Guittat, L.; Kaiser, M.; Sacca, B.; Amrane, S.; Bourdoncle, A.; Albertti, P.; Teulade-Fichou, M.-P.; Lacriox, L.; Mergny, J.-L. Fluorescence-based melting assays for studying quadruplex ligands. *Methods* **2007**, *42*, 183−195.

(46) Luu, K. N.; Phan, A. T.; Kuryavyi, V.; Lacroix, L.; Patel, D. J. Structure of the human telomere in K⁺ solution: an intramolecular (3 + 1) G-quadruplex scaffold. *J. Am. Chem. Soc.* **2006**, *128*, 9963−9970.

(47) Yang, D.-Y.; Chang, T.-C.; Sheu, S.-Y. Interaction between human telomere and a carbazole derivative: a molecular dynamics simulation of a quadruplex stabilizer and telomerase inhibitor. *J. Phys. Chem. A* **2007**, *111*, 9224−9232.

(48) Campbell, N. H.; Parkinson, G. N.; Reszka, A. P.; Neidle, S. Structural basis of DNA quadruplex recognition by an acridine drug. *J. Am. Chem. Soc.* **2008**, *130*, 6722−6724.

(49) Miyoshi, D.; Matsumura, S.; Nakano, S.; Sugimoto, N. Duplex dissociation of telomere DNAs induced by molecular crowding. *J. Am. Chem. Soc.* **2004**, *126*, 165−169.

(50) Oganesian, L.; Moon, I. K.; Bryan, T. M.; Jarstfer, M. B. Extension of G-quadruplex DNA by ciliate telomerase. *EMBO J.* **2006**, *25*, 1148−1159.

(51) Bhattacharjee, A. J.; Ahluwalia, K.; Taylor, S.; Jin, O.; Nicoludis, J. M.; Buscaglia, R.; Chaires, J. B.; Kornfilt, D. J. P.; Marquardt, D. J. S.; Yatsunyk, L. A. Induction of G-quadruplex DNA structure by Zn(II) 5,10,15,20-tetrakis(N-methyl-4-pyridyl)porphyrin. *Biochimie* **2011**, *93*, 1297−1309.

telomeric G-quadruplex dimers: effect of the spacer in the design of potent telomerase inhibitors. *PLoS One* **2012**, *7*, No. e39467.

(52) Read, M.; Harrison, R. J.; Romagnoli, B.; Tanious, F. A.; Gowan, S. M.; Reszka, A. P.; Wilson, W. D.; Kelland, L. R.; Neidle, S. Structure-based design of selective and potent G quadruplex-mediated telomerase inhibitors. *Proc. Natl. Acad. Sci. U.S.A.* **2001**, *98*, 4844−4849.

(53) Mergny, J. L.; Helene, C. G-Quadruplex DNA: a target for drug design. *Nat. Med.* **1998**, *4*, 1366−1367.

(54) Reed, J.; Gunaratnam, M.; Beltran, M.; Reszka, A. P.; Vilar, R.; Neidle, S. TRAP-LIG, a modified telomere repeat amplification protocol assay to quantitate telomerase inhibition by small molecules. *Anal. Biochem.* **2008**, *380*, 99−105.

(55) Frisch, M. J.; Trucks, G. W.; Schlegel, H. B.; Scuseria, G. E.; Robb, M. A.; Cheeseman, J. R.; Montgomery, J. A., Jr.; Vreven, T.; Kudin, K. N.; Burant, J. C.; Millam, J. M.; Iyengar, S. S.; Tomasi, J.; Barone, V.; Mennucci, B.; Cossi, M.; Scalmani, G.; Rega, N.; Petersson, G. A.; Nakatsuji, H.; Hada, M.; Ehara, M.; Toyota, K.; Fukuda, R.; Hasegawa, J.; Ishida, M.; Nakajima, T.; Honda, Y.; Kitao, O.; Nakai, H.; Klene, M.; Li, X.; Knox, J. E.; Hratchian, H. P.; Cross, J. B.; Bakken, V.; Adamo, C.; Jaramillo, J.; Gomperts, R.; Stratmann, R. E.; Yazyev, O.; Austin, A. J.; Cammi, R.; Pomelli, C.; Ochterski, J. W.; Ayala, P. Y.; Morokuma, K.; Voth, G. A.; Salvador, P.; Dannenberg, J. J.; Zakrzewski, V. G.; Dapprich, S.; Daniels, A. D.; Strain, M. C.; Farkas, O.; Malick, D. K.; Rabuck, A. D.; Raghavachari, K.; Foresman, J. B.; Ortiz, J. V.; Cui, Q.; Baboul, A. G.; Clifford, S.; Cioslowski, J.; Stefanov, B. B.; Liu, G.; Liashenko, A.; Piskorz, P.; Komaromi, I.; Martin, R. L.; Fox, D. J.; Keith, T.; Al-Laham, M. A.; Peng, C. Y.; Nanayakkara, A.; Challacombe, M.; Gill, P. M. W; Johnson, B.; Chen, W.; Wong, M. W.; Gonzalez, C.; Pople, J. A. *Gaussian 03*; Gaussian, Inc.: Wallingford, CT, 2004.

(56) Parkinson, G. N.; Lee, M. P.; Neidle, S. Crystal structure of parallel quadruplexes from human telomeric DNA. *Nature* **2002**, *417*, 876−880.

(57) Haider, S. M.; Parkinson, G. N.; Neidle, S. Structure of a G-quadruplex−ligand complex. *J. Mol. Biol.* **2003**, *326*, 117−125.

(58) Parkinson, G. N.; Ghosh, R.; Neidle, S. Structural basis for binding of porphyrin to human telomeres. *Biochemistry* **2007**, *46*, 2390−2397.

(59) Read, M. A.; Neidle, S. Structural characterization of a guanine-quadruplex ligand complex. *Biochemistry* **2000**, *39*, 13422−13432.